Barriers for asymmetric fission of multiply charged C_{60} fullerenes

H. Cederquist, J. Jensen, H. T. Schmidt, and H. Zettergren
Physics Department, Stockholm University, AlbaNova, S-106 91 Stockholm, Sweden

S. Tomita
Department of Physics and Astronomy, University of Aarhus, DK-8000, Århus C, Denmark

B. A. Huber and B. Manil
CIRIL/GANIL, rue Claude Bloch, Boîte Postale 5133, 14070 Caen Cedex 5, France

(Received 21 February 2003; published 30 June 2003)

We have measured kinetic energy releases in asymmetric fission, $C_{60}^{r+} \rightarrow C_{58}^{(r-1)+} + C_2^+$ ($r=6$–9) and evaporation $C_{60}^{r+} \rightarrow C_{58}^{r+} + C_2$ ($r=2,3$), following multiple-electron removal from C_{60} in He^{2+} and Xe^{17+} collisions at $3q$ keV ($q=2,17$). We used the recoil-ion momentum technique and limited the initial momentum distribution of the target molecules by collimation of the effusive C_{60} jet. This yielded a resolution of 3 meV for the final kinetic energies of the charged C_{58} fragments, mapped out as two-dimensional position distributions at the end of a linear time-of-flight mass spectrometer. The present results for asymmetric fission are in agreement with earlier ones deduced from time-of-flight C_2^+ peak-shape and sector-field $C_{58}^{(r-1)+}$-energy analysis. Model calculations treating $C_{58}^{(r-1)+}$ and C_2^+ as conducting spheres indicate that the autocharge-transfer process, which has been proposed to link asymmetric fission to neutral C_2 emission, most likely is inactive for all r. Using a charge-independent activation energy for C_2 emission from C_{60}^{r+} of $E_a=10$ eV, we deduce fission barriers indicating lower (semiempirical) and upper (model) C_{60}^{r+}-stability limits of $r=11$ and $r=18$, respectively.

DOI: 10.1103/PhysRevA.67.062719 PACS number(s): 34.70.+e

I. INTRODUCTION

Highly excited finite systems, such as clusters and large molecules, may relax in a variety of ways such as by emission of photons [1], electrons [2], and neutral smaller clusters, molecules, or atoms. Multiply charged systems may, in addition, decay through fission processes emitting charged rather than neutral fragments. Fission of charged clusters have been studied by many groups both experimentally and theoretically (see, for example, Refs. [3–12]). The Rayleigh stability limit against fission for charged objects is defined through the equality between the disruptive Coulomb force and the attractive cohesive force [13]. This limit was demonstrated experimentally for the first time only in recent studies of fission of charged microdroplets [14], while earlier difficulties with smaller objects have been related to their internal excitations before the decay.

It is obviously difficult to control the internal temperatures of collisionally ionized C_{60} molecules, since the fullerene samples are heated to temperatures around 500 °C before significant sublimation occurs and, in addition, further substantial heating may be induced by the collision process. However, slow highly charged ions are known to be able to capture many electrons from fullerenes already at large distances where they, via direct processes, only transfer small amounts of energies to the internal nuclear motion and electronic excitations [15,16]. Indeed, such collisions have been used to produce metastable or stable highly charged C_{60} ions as exemplified by the observations of C_{60}^{9+} by Jin *et al.* [17] and C_{60}^{10+} by Brenac *et al.* [18] using Bi^{44+} and Xe^{25+} ions, respectively. Quite recently, unambiguous observations of C_{60}^{12+}, produced through multiple absorption of infrared photons from a femtosecond laser, were made [19]. So far, no detailed understanding of this supressed fragmentation, which is surprising in view of the expected heating by the photon field, has been reached. Theoretical predictions for the C_{60} stability limit spread from $r=10$ by Cioslowski, Patchkovskii, and Thiel [20] to $r=13$ and $r=16$ by Bastug *et al.* [21] and Seifert, Gutierrez, and Schmidt [22], respectively.

In this work we report measurements of kinetic energy releases, E_{KER}, in asymmetric fission

$$C_{60}^{r+} \rightarrow C_{58}^{(r-1)+} + C_2^+ \tag{1}$$

and evaporative neutral C_2-emission processes

$$C_{60}^{r+} \rightarrow C_{58}^{r+} + C_2 \tag{2}$$

for $r=6$–9 and $r=2$, 3, respectively. The multiply charged fullerene ions of interest here are produced in $3q$ keV

$$A^{q+} + C_{60} \rightarrow A^{(q-r)+} + C_{60}^{r+} \rightarrow \cdots \tag{3}$$

collisions, where q and r are the charge states of the incident projectile and the fullerene before decay. In the experiment, we have used Xe^{17+} and He^{2+} projectiles, of which the former produced stable C_{60}^{r+} in high charge states at large distances, and the latter hot (fragmenting) C_{60}^{2+} and C_{60}^{3+} in closer collisions.

In 1995, Scheier, Dünser, and Märk [23] presented results on kinetic energy releases in asymmetric fission of C_{60}^{r+} ions ($r=2$–7) following multiple-electron impact. In this pioneering work [23] they further introduced the autocharge-transfer (ACT) mechanism, according to which asymmetric

fission starts out as a neutral C_2-emission process followed by electron transfer from C_2 at well-defined distances. Since then, this model has been used and discussed in many articles on fullerene fragmentation (see, e.g., Refs. [10,11,23–28]). However, Tomita *et al.* [28] argue that their E_{KER} values may be rationalized without the autocharge-transfer mechanism and that evaporation and asymmetric fission are independent and competing processes controlled by activation energies and fission barriers.

In the following section, we describe the present experimental technique and procedure, which uses the method of recoil-ion momentum analysis to deduce experimental kinetic energy releases for the postcollisional fragmentation processes. Section III is devoted to comparisons with earlier experimental results using different techniques and (partly) different excitation methods (ion or electron impact). In addition, we compare measurements of kinetic energy releases in neutral C_2-emission processes $C_{60}^{r+} \rightarrow C_{58}^{r+} + C_2$ for $r = 2,3$ with literature values by Matt *et al.* [29], finding again good agreement between fragmentation following collision with Xe^{17+}, He^{2+}, and electrons [29]. In Sec. IV, we compare our measurements with model calculations using the static model for over-the-barrier electron transfer between two conducting spheres of finite radii [30] to discuss whether the ACT process or the reaction (fission) barrier concept is most apropriate to describe asymmetric fission. Finally, we deduce upper and lower bounds of $r = 11$ and $r = 18$ for the stability limit of C_{60}^{r+}.

II. THE EXPERIMENTAL SETUP AND METHOD

The experimental work has been performed at the Manne Siegbahn Laboratory at Stockholm University. Beams of slow He^{2+} and Xe^{17+} ions were provided by means of the 14.4 GHz Electron Cyclotron Resonance (ECR) ion source. The experimental setup is shown schematically in Fig. 1, where slow projectile ion beams enter the interaction region and cross a collimated effusive C_{60} jet from an oven kept at 600 °C. This jet points in the same direction as the linear time-of-flight mass spectrometer used to analyze distributions of intact and fragmented C_{60} ions.

A 180° cylindrical energy analyzer separates different final projectile charge states as they hit different regions on the two-dimensional position-sensitive microchannel plate detector. A fast signal from this detector is used to trigger the extraction field pulse, which means that the extraction typically is switched on about 1 μs after the collision (slightly different for different projectiles). This pulse has a rise time of less than 100 ns, an amplitude of -100 V, and a duration of 100 μs. As can be seen in Fig. 1, the extraction voltage is applied to the first drift tube of the spectrometer, while the outer spectrometer case is kept on ground potential. The center of the projectile beam passes the extraction region at a distance of only 3 mm from the top of the grounded case, while the total length of the extraction region is 20 mm. The three last drift tubes were kept at constant voltages of $V_1 = -500$ V, $V_2 = -2000$ V, and $V_3 = -1000$ V. The voltage of the front of the position sensitive detector was -2700 V.

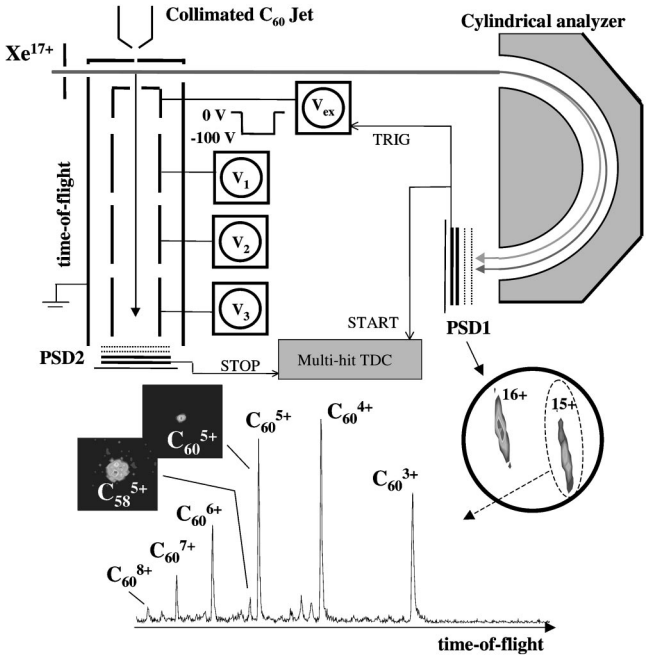

FIG. 1. A schematic of the setup for coincidence registration of final projectile charge states and intact/fragmented fullerene ions. An example of 50 keV Xe^{17+} ions colliding with C_{60} is shown. The analyzer voltage is set such that only Xe^{16+} and Xe^{15+} product ions hit the position sensitive detector (PSD1). The corresponding image on the detector is shown as an inset. The fullerene time-of-flight distribution coincident with the outgoing Xe^{15+} ions are also shown and for each one of the peaks in this spectrum there is a corresponding image on PSD2. Examples are displayed for C_{60}^{5+} and C_{58}^{5+}.

The cylindrical analyzer is only focusing in the horizontal plane and it is therefore possible to measure projectile angular scattering distributions [15]. Here, we will, however, focus on the coincidence registration (list mode) of the final projectile charge state and the final charge and mass of ionized intact or fragmented C_{60}. An example is shown in Fig. 1 for the specific case in which two electrons are stabilized on incident Xe^{17+} projectiles. These collisions ($Xe^{17+} \rightarrow Xe^{15+}$) produce mostly intact C_{60}^{r+} ions in charge states $r = 2$–9 (the $r = 2$ and $r = 9$ peaks are not shown in the spectrum). Large fullerene fragments (C_{60-2m}) with rather low intensities are produced in charge states larger than or equal to three and even numbers of carbon atoms ($60-2m = 58,56,54,\ldots$). The time-of-flight peaks are associated with position distributions, which are characteristic for kinetic energy releases in the fragmentation processes.

In Fig. 2, we show position distributions for intact C_{60} and C_{58} fragments in final charge states 4, 5, and 6. The *fragment* images become wider with increasing charge (and also with increasing numbers of lost C_2 units [31]). Note that the time scales for the fragmentation processes are much longer (at least of the order of picoseconds) than the collision times ($\sim$10 fs), but also, in general, much shorter than the time (of the order of 10 μs) it takes the ions to leave the extraction region. Decay on time scales comparable to, or larger than, the extraction time would result in distortions and shifts of the corresponding time-of-flight peaks.

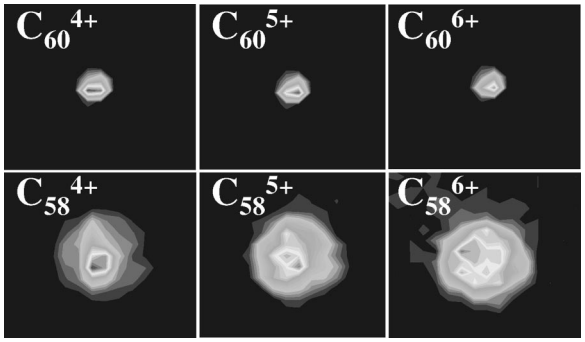

FIG. 2. Position images on the recoil detector for intact C_{60}^{r+} ions with $r=4,5,6$ (upper row) and C_{58} ions resulting from fragmentation (lower row). The latter images demonstrate the influences of kinetic energy releases in connection with the postcollisional fragmentation of C_{60} following interaction with 50 keV Xe^{17+} ions. The dimensions of the detector images are 7×7 mm^2, which are only smaller parts of the whole detector area (50 mm in diameter).

The fragment kinetic energy release scale is calibrated by introducing room temperature Xe gas in the interaction region. The single-electron capture process $Xe^{17+}+Xe \rightarrow Xe^{16+}+Xe^{+}$ is dominated by large impact parameters and can thus be shown to transfer only a negligible amount of additional momentum to the Xe target. The 300 K Maxwellian velocity distribution thus directly yields the position distribution on the target detector. As can be seen in Fig. 3 (showing zoom-ins on target position distributions), the thermal Xe target gas gives a detector image, which is several times larger than the image due to single-electron capture from a C_{60} molecule in the effusive jet. The very small C_{60}^{+} image is due to the jet collimation, which strongly limits the initial velocity distribution perpendicular to the spectrometer axis. In the following we will assume linear relations between perpendicular ion velocities and the radial positions for hits on the detector; that is, abberations in the (weak) lenses of the time-of-flight spectrometer are neglected, which is quite reasonable as the ion trajectories are rather close to the spectrometer axis even for the largest (fragment) velocities dealt with here. The kinetic energy release for a certain fragmentation process then becomes

$$E_{\mathrm{KER}}=30E_{\mathrm{therm}}\left[\frac{\Delta_{C_{58}^{(r+)}}}{\Delta_{Xe^{+}}}\frac{t_{Xe^{+}}}{t_{C_{58}^{(r+)}}}\right]^{2}\frac{m_{C_{58}}}{m_{Xe}}, \qquad (4)$$

where $\Delta_{C_{58}^{(r+)}}$ and $\Delta_{Xe^{+}}$ are the widths of the projected position distributions (deconvoluted by the narrow instrumental widths as given by the images for intact fullerenes). The flight times are denoted $t_{Xe^{+}}$ and $t_{C_{58}^{(r+)}}$, and $E_{\mathrm{therm}}=38$ meV is the average kinetic energy for the thermal Xe gas before the collision. The resolution in E_{KER} for C_2 emission is roughly 90 meV, which is $60/2=30$ times larger than the ~3 meV instrumental resolution measured through the relation between the widths of the peaks for intact C_{60}^{+} and Xe^{+} [cf. Fig. 3 and Eq. (4)].

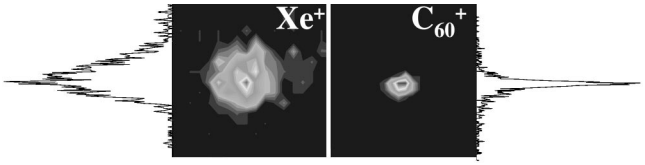

FIG. 3. Left: A 8×8 mm^2 zoom-in on the two-dimensional image of Xe^{+} target ions produced in 50 keV $Xe^{17+}+Xe\rightarrow Xe^{16+}+Xe^{+}$ single-electron capture collisions where the Xe target gas had a temperature of 300 K. Right: A similar zoom-in on the two-dimensional image of C_{60}^{+} target ions produced in 50 keV $Xe^{17+}+C_{60}\rightarrow Xe^{16+}+C_{60}^{+}$ single-electron capture collisions with a collimated C_{60} jet (cf. text). Projected position distributions are also shown.

III. RESULTS AND COMPARISONS

In Fig. 4 we show the measured E_{KER} values for the process where C_{60}^{r+} emits a single C_2^{+} molecule as a function of the final C_{58} fragment charge state. This is compared with measurements using different methods such as the MIKE (Mass-analyzed Ion Kinetic Energies) and TOF (time-of-flight) techniques. In the MIKE-scan technique [23–25,29], the energy distribution of the selected heavy fragments (C_{58} ions) are measured by means of an electrostatic analyzer, and from their widths, the E_{KER} values are determined [23–25]. In the TOF technique [27,28], the energy distribution of the C_2^{+} fragments were obtained from peak-shape analysis of the C_2^{+} peaks. In those measurements, the primary C_{60} ions were produced by slow highly charged ion impact, whereas the MIKE-scan measurements used electron impact to ionize the C_{60} molecules.

In the measurements by Scheier, Dünser, and Märk [23], Senn, Märk, and Scheier [25], Chen *et al.* [27], and Tomita *et al.* [28], the experimentally selected dissociation process is that of pure asymmetric fission, of the type given by Eq. (1). Our values are close to the fission data from Refs. [23] and [28] for final C_{58} charge states 5 and 6, and 5–7, respec-

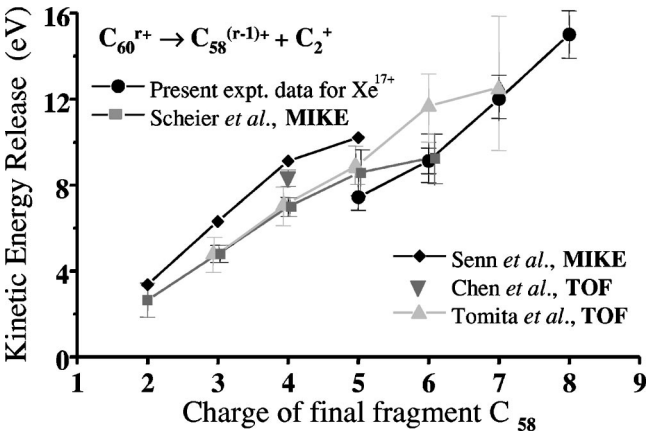

FIG. 4. Experimental kinetic energy releases for the process where C_{60}^{r+} emits a single C_2^{+} molecule compared with earlier measurements based on other methods, such as the MIKE technique by Scheier, Dünser, and Märk [23], and Senn, Märk, and Scheier [25], and the TOF technique by Chen *et al.* [27] and Tomita *et al.* [28] (cf. text).

TABLE I. Experimental kinetic energy releases (in units of eV) for the asymmetric fission processes $C_{60}^{r+} \rightarrow C_{58}^{(r-1)+} + C_2^+$.

C_{60}^{r+}	$r=6$	$r=7$	$r=8$	$r=9$
E_{KER}	7.4 ± 0.4	9.1 ± 0.5	12.0 ± 1.0	15.0 ± 1.1

tively. The results of Senn, Märk, and Scheier [25], for which no error bars are given, lie above all other measurements. Purely evaporative processes [Eq. (2)] are selected in the measurements by Matt *et al.* [29], yielding much lower E_{KER} values than for fission. In our measurements we see large contributions from evaporation of neutral C_2 units, for final charges of C_{58} ions lower than 5. Our measured kinetic energy release for C_2 emission from C_{60}^{3+} are 0.9 ± 0.3 and 0.5 ± 0.2 eV following 6 keV He^{2+} and 34 keV Xe^{17+} impact, respectively. The latter measurements are in agreement with the evaporation values, around 0.4 eV, by Matt *et al.* [29]. These comparisons demonstrate that the present technique is applicable for large and small values of the kinetic energy releases. The present low E_{KER} value, 2.0 ± 0.2, derived from the measured C_{58}^{4+} width, as compared to those obtained for asymmetric fisson suggests that our C_{58}^{4+} ions originate predominantly from evaporation of a neutral C_2 from C_{60}^{4+} and not from the fission of C_{60}^{5+}. This is qualitatively in good agreement with the results of Martin *et al.* [32] and Chen *et al.* [33], who measured dominance of evaporation over fission for the decay of C_{60}^{4+} produced in collisions, stabilizing two electrons on Ar^{8+} and Xe^{8+} projectiles. In Table I we summarize the present kinetic energy release measurements for asymmetric fission [Eq. (1)]. The error bars, ranging from ± 0.4 to ± 1.1 eV, are dominated by statistical uncertainties in the measured widths of the detector images, while the intrinsic instrumental E_{KER} resolution is about ± 0.1 eV (cf. above).

IV. DISCUSSIONS

A. Kinetic energy releases and the autocharge-transfer process

For the purpose of discussions of the kinetic energy release measurements, we use a simple model in which we treat the two separating fragments as conducting spheres. This model was first developed by Näher *et al.* [5] in 1997 and in 2002 Zettergren *et al.* [30] presented a partly extended version, taking the effect of electron transfer during fragmentation into account. The latter effect is the basis of the ACT process in which it is assumed that the fragmentation starts out as a separation in a charged heavy (C_{58}) and light (C_2) neutral fragment, which at some fairly large critical distance loses an electron to the charged fragment [23,24].

In Fig. 5, we show calculated potential energy curves for the $C_{60}^{r+} \rightarrow C_{58}^{(r-1)+} + C_2^+$ and the $C_{60}^{r+} \rightarrow C_{58}^{r+} + C_2$ fragmentation processes for $r=2$, $r=3$, $r=4$, and $r=5$, using the method described by Zettergren *et al.* [30]. Here, we have assumed that the radius of the heavy fragment is given by $a_{C_{58}} = a_{C_{60}}(1-2m/60)^{1/2} = 7.1a_0$, i.e., that C_{58} and C_{60} have the same surface densities. The C_{60} radius $a_{C_{60}} = 7.2a_0$ was obtained independently by fitting the expression for the ionization of a metal sphere [30,34], $I_r(C_{60}) = W + (r-1/2)/a_{C_{60}}$, to experimental ionization potentials for C_{60} [30]. The radius, $a_{C_2} = 2.4a_0$, of the C_2 fragment is deduced from $I_1(C_2) = W + 1/(2a_{C_2})$ and the accepted experimental I_1 value of 11.4 ± 0.4 eV [35]. In Fig. 5, the potential energies are set to zero for asymmetric fission at infinite center-center distances R. The energy separations between these potential curves and the corresponding ones for (neutral) C_2 emission at $R=\infty$ are taken to be $I_r(C_{58}) - I_1(C_2)$, where $I_r(C_{58}) = W + (r-1/2)/a_{C_{58}}$. This sequence of ionization potentials for C_{58} are close to those calculated by Martin *et al.* [11] and Seifert, Vietze, and Schmidt [36].

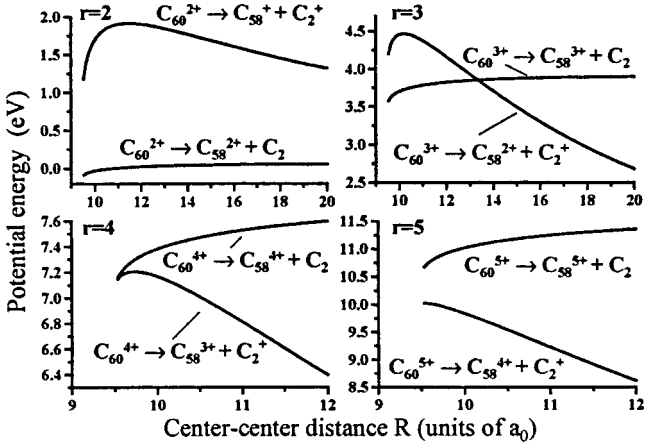

FIG. 5. The interaction energies for two conducting spheres used to model the $C_{58}^{(r-1)+} + C_2^+$ and $C_{58}^{r+} + C_2$ intermolecular potentials as functions of R for $r=2$, 3, 4, and 5. The potential energies for fission (C_2^+ emission) approach zero as R approaches infinity. The calculations are started at minimum values slightly larger than $a_{C_{58}} + a_{C_2}$. Note the differences in energy and distance scales in the four figures!

From the upper left Fig. 5 it is obvious that it is energetically more favorable to emit a neutral than a charged C_2 unit within the present sphere-sphere interaction model for C_{60}^{2+}. For $r=3$, the two potential energy curves cross around $R = 14.5a_0$, which is outside the critical distance for electron transfer at $R_c = 12.7a_0$. This means that although the potential energies of the sphere-sphere system are the same for asymmetric fission and evaporation at $14.5a_0$, the potential barrier, which the electron experiences as it attempts to move from the lighter to the heavier sphere, is higher than its total energy. Under these circumstances, the ACT process would require tunneling through a thick barrier and is probably not very efficient. The experimental results indeed clearly shows that neutral C_2 emission is dominant for C_{60}^{3+}.

The lower left and lower right parts of Fig. 5 show that the fission potential energy curves lie below those for evaporation for all R and thus there is no crossing, and direct C_2^+ emission should become dominant for $r=4$ and $r=5$. The same is true for $r>5$, as can be seen in Fig. 6. Thus, from pure model considerations we would conclude that the ACT process—most likely—is inactive for all r. The curve cross-

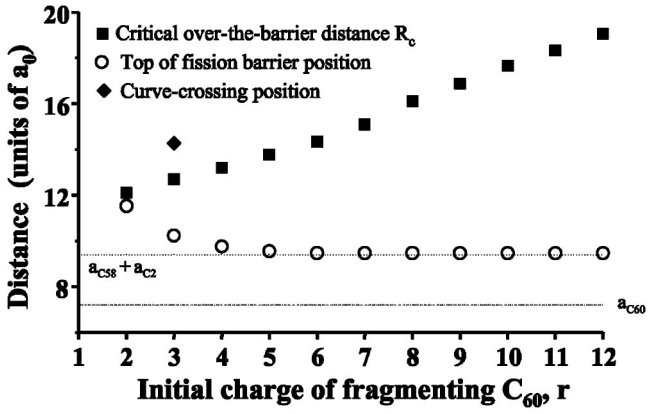

FIG. 6. The critical distances R_c for over-the-barrier electron transfer from the a_{C2} sphere as functions of r (filled squares), the positions in R (center-center distance) for the maxima of the model $C_{58}{}^{(r-1)+}-C_2{}^+$ potentials (open circles), and the positions (in R) of the crossings between the model potentials for neutral C_2 and charged $C_2{}^+$ emission. Note that such a crossings only exists for $r=3$ and that the fission barrier height thus is expected to control the decay rate for $r\geqslant 4$.

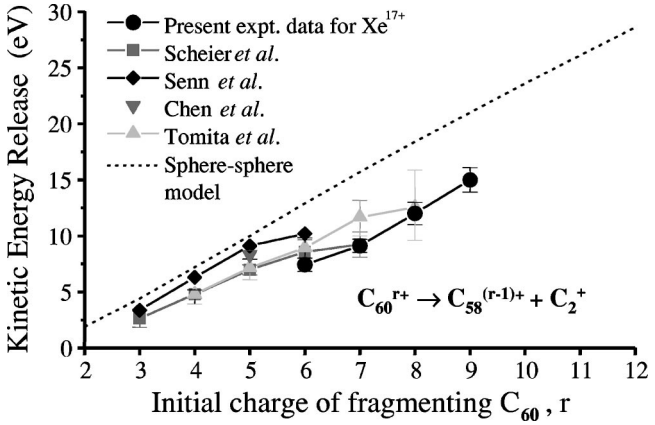

FIG. 7. Experimental (Scheier, Dünser, and Märk [23], Senn, Märk, and Scheier [25], Chen *et al.* [27], Tomita *et al.* [28]) and calculated kinetic energy releases for the fission process where a $C_{60}{}^{r+}$ ion emits a single $C_2{}^+$ ion. The present sphere-sphere model results are due to the interactions between two polarizable spheres of finite radii.

ing positions, however, depend strongly on the assumed values of the C_{58} ionization potentials, especially in the $C_{60}{}^{4+}$ case, where shifts well below 1 eV may provide a crossing at a suitable distance inside the critical distance for electron transfer at $R_c=13.2a_0$.

The present sphere-sphere model E_{KER} values, taken as the maxima of the calculated potential energy curves for the fission process $C_{60}{}^{r+}\rightarrow C_{58}{}^{(r-1)+}+C_2{}^+$, are shown in Fig. 7 together with various experimental results. In the model it is assumed that fission products are in their electronic and vibrational ground states. This is not the case in the experimental situation, since the $C_{60}{}^{r+}$ ions are excited before fragmentation, partly due to the heating in the oven, and partly due to the collision process. This and the fragmentation process itself most likely result in a final vibrationally excited state, yielding a smaller difference in relation to the maximum of the potential energy barrier, and thereby smaller E_{KER} values, as indicated in Fig. 8.

B. Fission barriers and C_{60} stability limits

As shown schematically in Fig. 8, the kinetic energy releases E_{KER} in asymmetric fission relates to the fission barriers B^r_{fis} through

$$B^r_{\mathrm{fis}}=E_{\mathrm{KER}}+E^r_a+I_1(\mathrm{C}_2)-I_r(\mathrm{C}_{58}), \tag{5}$$

or alternatively

$$B^r_{\mathrm{fis}}=E_{\mathrm{KER}}+E^{r-1}_a+I_1(\mathrm{C}_2)-I_r(\mathrm{C}_{60}), \tag{6}$$

under the assumption that the fragmentation products are in their ground states ($E_{\mathrm{exc}}=0$). The activation energies for neutral C_2 emission (evaporation) from $C_{60}{}^{(r-1)+}$ and $C_{60}{}^{r+}$ are denoted by E^{r-1}_a and E^r_a, respectively. The exact value of the C_2 activation energy for neutral C_{60} has been the subject of a rather long debate with reported experimental values ranging between 3 and 15 eV [37]. Recently, however, Tomita *et al.* [1] presented results for dissociation from $C_{60}{}^+$ using an electrostatic ion storage ring, and by taking the difference between the first ionization potentials for C_{60} and C_{58} into account they arrived at $E_a(\mathrm{C}_{60})=10.3\pm 0.1$ eV [1]. This is consistent with the results by Matt *et al.* [37] who reevaluated a rather large set of earlier data.

The relations between the C_2 dissociation energies for neutral and charged C_{60} are linked by the relations between the ionization potentials for C_{60} and C_{58} through

$$E^r_a=E_a(\mathrm{C}_{60})+\sum_{k=1}^{r}\left[I_k(\mathrm{C}_{58})-I_k(\mathrm{C}_{60})\right]. \tag{7}$$

Unfortunately, there are only a limited amount of experimental data available for ionization potentials and dissociation energies. The C_2 dissociation energies for $C_{60}{}^{r+}$ have been measured for $r=0-3$ [1,37,38] and for C_{58} and C_{60} there

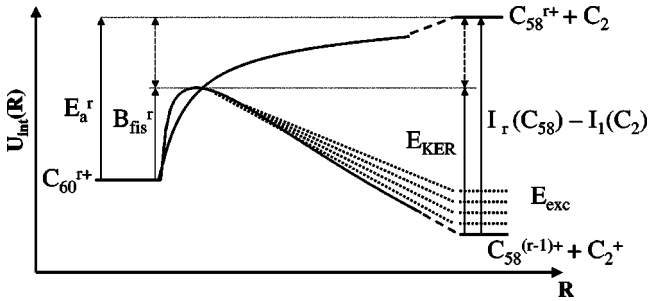

FIG. 8. A schematic of the relation between the fission barrier for $C_2{}^+$ emission from $C_{60}{}^{r+}$, B^r_{fis}, the rth ionization potential for C_{58}, $I_r(C_{58})$, the ionization potential for C_2, $I_1(C_2)$, the kinetic energy release E_{KER} for fission products in their ground states, and the activation energy for C_2 emission from $C_{60}{}^{r+}$, E^r_a. Noting that the two double arrows represent the same energy we arrive at the expression $B^r_{\mathrm{fis}}=E_{\mathrm{KER}}+E^r_a+I_1(\mathrm{C}_2)-I_r(\mathrm{C}_{58})$. E_{exc} denotes the possible vibrational excitation after fragmentation (cf. text).

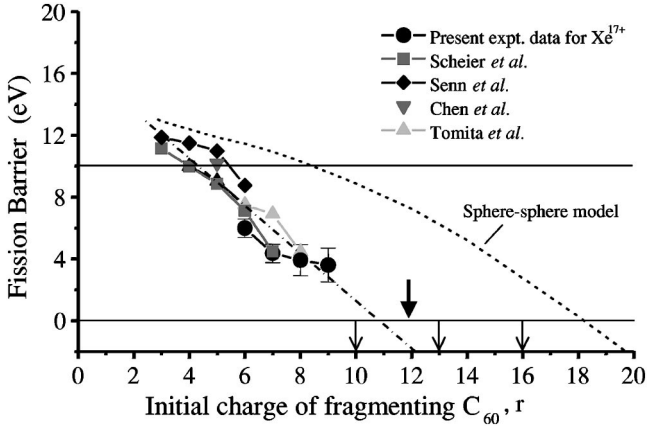

FIG. 9. Semiempirical (based on the present E_{KER} values and Scheier, Dünser, and Märk [23], Senn, Märk, and Scheier [25], Chen *et al.* [27], and Tomita *et al.* [28]) and model fission barriers for the $C_{60}^{r+} \rightarrow C_{58}^{(r-1)+} + C_2^+$ process. The curves show: a fit to experimental data and the present sphere-sphere model results. Error bars are only shown for the present experimental results. The line at 10 eV shows the assumed activation energy for neutral C_2 emission. Theoretical predictions of the stability limit are indicated by arrows ($r=10$; Cioslowski, Patchkovskii, and Thiel [20], $r=13$; Bastug *et al.* [21] and $r=16$; Seifert, Gutierrez, and Schmidt [22]). The thick arrow shows the highest observed C_{60} charge state $r=12$ [19].

are only measurements for the first [39] and for the first four [40] ionization potentials, respectively.

Sequences of ionization potentials have been calculated for both C_{58} and C_{60}, but never for sufficiently large r within the same theoretical framework. To our knowledge, the most advanced calculations up to now are those by Bastug *et al.* [21] and Yannoulas and Landman [41] for C_{60}^{r+} with $r=1-8$ and $r=1-12$, respectively, and those by Martin [42] for C_{60}^{r+} and C_{58}^{r+} with $r=0$, 1, and 2. Further, Martin *et al.* [11] have recently calculated C_{58} ionization potentials using the GAUSSIAN code [11]. The calculations [42] yield dissociation energies E_a^r, which are about 12.5 eV, 11.8 eV, and 11.3 eV for $r=0$, 1, and 2, respectively. This is the trend expected from the formula above as C_{60} probably has higher ionization potentials than C_{58} due to its higher symmetry. Here, we will, however, due to lack of sufficient experimental or theoretical data, follow earlier conventions and make the assumption that the C_2-dissociation energy is independent of r and set it to $E_a=10$ eV.

In Fig. 9, we show semiempirical and model fission barriers for C_2^+ emission from C_{60}^{r+} as functions of r, as calculated with Eq. (5). For the former results we have used the present measurements of kinetic energy releases and those by Scheier, Dünser, and Märk [23], Senn, Märk, and Scheier [25], Chen *et al.* [27], and Tomita *et al.* [28], and the ionization potentials of C_2 and C_{58} as calculated by Martin *et al.* [11]. The model fission barriers are obtained by using the very same values of E_a, $I_1(C_2)$, and $I_r(C_{58})$ and the full sphere-sphere interaction model (yielding exact expressions for the mutual polarizations of two spheres of finite radii [30]). This gives an upper stability limit of $r=18$ (see Fig. 9).

The semiempirical fission barrier results, however, point at a much lower limit of $r=11$. Here, we should remember that the semiempirical results should be regarded as lower limits for the fission barriers, as vibrational excitations of the fragments after the decay are neglected. The most highly charged intact C_{60} molecule, which has been observed experimentally is C_{60}^{12+}, produced by multiphoton absorption [19]. Theoretical predictions are indicated by arrows in Fig. 9 [20–22]. The theoretical results by Bastug *et al.* [21] and Seifert, Gutierrez, and Schmidt [22] fall within the range indicated by the present work.

V. CONCLUSION

In the present work, we have presented a technique to measure kinetic energy releases in $C_{60}^{r+} \rightarrow C_{58}^{(r-1)+} + C_2^+$ and $C_{60}^{r+} \rightarrow C_{58}^{r+} + C_2$ fragmentation processes. We achieved a resolution of 3 meV in the measurements of the final C_{58} kinetic energies, using a collimated effusive C_{60} jet pointing along the axis of a linear time-of-flight spectrometer terminated by a two-dimensional position sensitive detector. Experimental results on the fission (C_2^+-emission) and evaporation (C_2-emission) processes are in good agreement with earlier results, using quite different experimental techniques. Considering the (unknown) vibrational energies of the $C_{58}^{(r-1)+}$ fragments, our measured kinetic energy releases appear as reasonable lower bounds to the predictions of a simple model, neglecting such excitations and treating the fragmentations as electrostatic interactions between two conducting spheres of finite radii. Fission barriers are deduced from the present experimental and model results, indicating lower and upper bounds for the stability limit of charged C_{60}^{r+} of $r=11$ and $r=18$, bracketing theoretical predictions by Bastug *et al.* [21] and Seifert, Gutierrez, and Schmidt [22]. We further conclude that ACT process most likely is inactive in asymmetric fission of C_{60}^{r+}. Instead it appears that evaporation and asymmetric fission, in general, are independent processes governed by the fission barrier and the activation energy for neutral C_2 emission. High-level calculations of ionization-potential sequences (for C_{58} and C_{60}) and charge dependent C_2 activation energies are obviously urgently needed for better understanding of fullerene fragmentation and stability.

ACKNOWLEDGMENTS

Discussion with Professor Fernando Martin, Universidad Autonoma de Madrid, and Professor Burkhard Fricke, University of Kassel, are gratefully acknowledged. We are also grateful to Patrik Löfgren, Mikael Blom, and Mikael Björkhage at the Manne Siegbahn Laboratory for highly valuable technical assistance. This work was supported by the Swedish Research Council through Contract Nos. F650-19981278 and F5102-993/2001. The present collaboration is part of the Low Energy Ion Beam Facilities (LEIF) European network HPRI-CT-1999-40012. This work was also supported by the Danish National Research Foundation through the Aarhus Center for Advanced Physics (ACAP).

[1] S. Tomita, J.U. Andersen, C. Gottrup, P. Hvelplund, and U.V. Pedersen, Phys. Rev. Lett. **87**, 073401 (2001).
[2] J.U. Andersen, P. Hvelplund, S.B. Nielsen, U.V. Pedersen, and S. Tomita, Phys. Rev. A **65**, 053202 (2002).
[3] U. Näher, S. Frank, N. Malinowski, U. Zimmerman, and T.P. Martin, Z. Phys. D: At., Mol. Clusters **31**, 191 (1994).
[4] C. Brechignac, Ph. Cahuzac, F. Carlier, M. de Frutos, R.N. Barnett, and U. Landman, Phys. Rev. Lett. **72**, 1636 (1994).
[5] U. Näher, S. Bjørnholm, S. Frauendorf, F. Garcias, and C. Guet, Phys. Rep. **285**, 245 (1997).
[6] S. Krückeberg, G. Dietrich, K. Lützenkirchen, L. Schweikhard, and J. Ziegler, Phys. Rev. A **60**, 1251 (1999).
[7] S. Martin, L. Chen, A. Denis, R. Brédy, J. Bernard, and J. Désesquelles, Phys. Rev. A **62**, 022707 (2000).
[8] F. Chandezon, S. Tomita, D. Cormier, P. Grübling, C. Guet, H. Lebius, A. Pesnelle, and B.A. Huber, Phys. Rev. Lett. **87**, 153402 (2001).
[9] E.E.B. Campbell, K. Hansen, K. Hoffmann, G. Korn, M. Tchaplyguine, M. Wittmann, and I.V. Hertel, Phys. Rev. Lett. **84**, 2128 (2000).
[10] L. Chen, S. Martin, R. Brédy, J. Bernard, and J. Désesquelles, Europhys. Lett. **58**, 375 (2002).
[11] S. Martin, L. Chen, R. Bredy, J. Bernard, M.C. Buchet-Poulizac, A. Allouche, and J. Désesquelles, Phys. Rev. A **66**, 063201 (2002).
[12] S. Tomita, H. Lebius, A. Brenac, F. Chandezon, and B.A. Huber, Phys. Rev. A **65**, 053201 (2002).
[13] Lord Rayleigh, Philos. Mag. **14**, 184 (1882).
[14] D. Duft, H. Lebius, B.A. Huber, C. Guet, and T. Leisner, Phys. Rev. Lett. **89**, 084503 (2002).
[15] H. Cederquist, A. Fardi, K. Haghighat, A. Langereis, H.T. Schmidt, S.H. Schwartz, J.C. Levin, I.A. Sellin, H. Lebius, B.A. Huber, M. O. Larsson, and P. Hvelplund, Phys. Rev. A **61**, 022712 (2000).
[16] A. Langereis, J. Jensen, A. Fardi, K. Haghighat, H.T. Schmidt, S.H. Schwartz, H. Zettergren, and H. Cederquist, Phys. Rev. A **63**, 062725 (2001).
[17] J. Jin, H. Khemliche, M.H. Prior, and Z. Xie, Phys. Rev. A **53**, 615 (1996).
[18] A. Brenac, F. Chandezon, H. Lebius, A. Pesnelle, S. Tomita, and B.A. Huber, Phys. Scr., T **80**, 195 (1999).
[19] V. R. Bhardwaj, M. Smits, A. Stolow, P. B. Corkum, and D.M. Rayner, in Book of Abstracts for the 11th International Conference on the Physics of Highly Charged Ions, Caen, France, September 2002 (unpublished), p. 192.
[20] J. Cioslowski, S. Patchkovskii, and W. Thiel, Chem. Phys. Lett. **248**, 116 (1996).
[21] T. Bastug, P. Kurpick, J. Meyer, W.D. Sepp, B. Fricke, and A. Rosen, Phys. Rev. B **55**, 5015 (1997).
[22] G. Seifert, R. Gutierrez, and R. Schmidt, Phys. Lett. A **211**, 357 (1996).
[23] P. Scheier, B. Dünser, and T.D. Märk, Phys. Rev. Lett. **74**, 3368 (1995).
[24] T.D. Märk and P. Scheier, Nucl. Instrum. Methods Phys. Res. B **98**, 469 (1995).
[25] G. Senn, T.D. Märk, and P. Scheier, J. Chem. Phys. **108**, 990 (1998).
[26] P. Scheier, G. Senn, S. Matt, and T.D. Märk, Int. J. Mass Spectrom. Ion Processes **172**, L1 (1998).
[27] L. Chen, J. Bernard, G. Berry, R. Brédy, J. Désesquelles, and S. Martin, Phys. Scr., T **92**, 138 (2001).
[28] S. Tomita, H. Lebius, A. Brenac, F. Chandezon, and B. A. Huber, Phys. Rev. A (to be published).
[29] S. Matt, M. Sonderegger, R. David, O. Echt, P. Scheier, J. Laskin, C. Lifshitz, and T.D. Märk, Int. J. Mass. Spectrom. **185**, 813 (1999).
[30] H. Zettergren, H.T. Schmidt, H. Cederquist, J. Jensen, S. Tomita, P. Hvelplund, H. Lebius, and B.A. Huber, Phys. Rev. A **66**, 032710 (2002).
[31] J. Jensen, H. Zettergren, A. Fardi, H. T. Schmidt, and H. Cederquist, Nucl. Intrum. Methods Phys. Res. B **205**, 643 (2003).
[32] S. Martin, L. Chen, A. Denis, and J. Désesquelles, Phys. Rev. A **57**, 4518 (1998).
[33] L. Chen, J. Bernard, A. Denis, S. Martin, and J. Désesquelles, Phys. Rev. A **59**, 2827 (1999).
[34] W.A. deHeer and P. Milani, Phys. Rev. Lett. **65**, 3356 (1990).
[35] C.J. Reid, J.A. Ballestine, S.R. Andrews, and F.M. Harris, Chem. Phys. Lett. **190**, 113 (1995).
[36] G. Seifert, K. Vietze, and R. Schmidt, J. Phys. B **29**, 5183 (1996).
[37] S. Matt, O. Echt, P. Scheier, and T.D. Märk, Chem. Phys. Lett. **348**, 194 (2001).
[38] S. Matt, O. Echt, M. Sonderegger, R. David, P. Scheier, J. Laskin, C. Lifshitz, and T.D. Märk, Chem. Phys. Lett. **303**, 379 (1999).
[39] J.A. Zimmermann, J.R. Eyler, S.B.H. Bach, and S.W. McElvany, J. Chem. Phys. **94**, 3356 (1991).
[40] C. Javahery, A. Wineel, S. Petrie, and D.K. Bohme, Chem. Phys. Lett. **204**, 467 (1993).
[41] C. Yannouleas and U. Landman, Chem. Phys. Lett. **217**, 175 (1994).
[42] Fernando Martin (private communication).